

## Supporting Information

### Layer-by-layer Assembly of Thick, Cu<sup>2+</sup>-Chelating Films

Salinda Wijeratne, Merlin L. Bruening\* and Gregory L. Baker<sup>†</sup>

<sup>a</sup>*Department of Chemistry, Michigan State University, East Lansing, Michigan 48824, USA*

\*Corresponding author.

<sup>†</sup>Professor Baker passed away unexpectedly on October 17, 2012. We dedicate this work as a memorial to him.

**Table S1.** Contact angles on (PAH/PDCMAA)<sub>10</sub> films deposited at different pH values.

**Table S2.** Contact angles on (PAH/PDCMAA)<sub>10</sub>/PAH films deposited at different pH values.

**Table S3.** Changes in thickness after adsorption of each polyelectrolyte layer during deposition of (PAH/PDCMAA)<sub>n</sub> films at different pH values.

**Figure S1.** <sup>1</sup>H NMR spectra of (a) poly(allylamine hydrochloride) (PAH) in D<sub>2</sub>O and (b) poly[(*N,N*-dicarboxymethyl)allylamine] in D<sub>2</sub>O adjusted to pH >10 by addition of NaOD. (c) <sup>13</sup>C NMR spectra of PAH (bottom) and PDCMAA (top). Both spectra were acquired in D<sub>2</sub>O adjusted to pH 10 by addition of NaOD. In the <sup>13</sup>C NMR spectrum of PDCMAA, the signal due to the carbons in the polymer backbone is likely low due to restricted relaxation.

**Figure S2.** IR spectra of (a) a (PAH/PDCMAA)<sub>10</sub>-Cu<sup>2+</sup> film on Au (reflectance spectrum), (b) a (PAH/PDCMAA)<sub>10</sub> film on Au (reflectance spectrum), (c) PDCMAA (in KBr) and (d) PAH (in KBr). Absorbance scales are not the same for all spectra.

**Figure S3.** Acid-base titration curves for 0.05 M NaOH (black-squares), ~0.022 M PAH in 0.05 M NaOH (red-squares) and ~0.022 M PDCMAA in 0.05 M NaOH (blue-squares). The titrant contained 1.0 M HCl.

**Figure S4.** Images of water droplets on the surfaces of (PAH/PDCMAA)<sub>10</sub> films assembled at pH (a) 3.0, (b) 5.0, (c) 7.0 and (d) 9.0. Values of  $\theta$  represent the average contact angle determined from the image.

**Figure S5.** Total surface energies, polar ( $\gamma_s^p$ ) and non-polar ( $\gamma_s^d$ ) components of surface energies, and thicknesses of (PAH/PDCMAA)<sub>10</sub> films assembled at different pH values.

**Figure S6.** Ellipsometrically determined refractive indices (549 nm) for (PAH/PDCMAA)<sub>n</sub> films deposited at pH 3.0, 5.0, 7.0 and 9.0. Integer numbers of bilayers indicate films terminated with PDCMAA deposition (blue squares) and fractional numbers represent terminal PAH deposition (red squares). Films with fewer layers did not give reliable values for refractive indices because of their low thickness.

**Figure S7.** Ellipsometric thicknesses and refractive indices (549 nm) of (PAH/PDCMAA)<sub>10</sub> films assembled at different pH values.

**Figure S8.** Ellipsometric thicknesses and refractive indices of PAH/PDCMAA films deposited at pH 3.0 and stored in ambient air or dried in vacuo for 24 h. (Thicknesses were measured within 2 min after removing the substrate from the vacuum chamber.)

**Figure S9.** (a) Swelling percentages and (b) water volume fractions and refractive indices for (PAH/PDCMAA)<sub>10</sub> films assembled at different pH values and immersed in pH 4.0 water. Figure (b) gives the refractive indices of “dry” films (ambient conditions) for comparison.

**Figure S10.** “Dry” (ambient conditions) thicknesses of (PAH/PDCMAA)<sub>n</sub> films adsorbed at (a) pH 3.0, (b) pH 5.0, (c) pH 7.0 and (d) pH 9.0. Fractional values of *n* (0.5, 1.5, 2.5, etc.) indicate terminal adsorption of PAH, whereas integers corresponds to terminal adsorption of PDCMAA.

**Figure S11.** Changes in film thickness,  $\delta d$ , after the deposition of each layer in (PAH/PDCMAA)<sub>n</sub> films formed at (a) pH 3.0, (b) pH 5.0, (c) pH 7.0, and (d) pH 9.0. Blue and red circles show the increase in thickness after adsorption of PDCMAA and PAH, respectively.

**Figure S12.** Reflectance IR spectra (2200-800 cm<sup>-1</sup>) of (PAH/PDCMAA)<sub>n</sub> films deposited on MPA-modified Au at (a) pH 3.0 (b) pH 5.0, (c) pH 7.0 and (d) pH 9.0. Films were rinsed with deionized water and dried with N<sub>2</sub> prior to obtaining the spectra. In each graph, the number of bilayers in the film increase from *n*=1 (bottom, black line) to 10 (top, olive green). The large –COO<sup>-</sup> stretch (relative to the acid carbonyl stretch) shows that after rinsing with water most –COOH groups are deprotonated.

**Figure S13.** AFM 3D images of (PAH/PDCMAA)<sub>10</sub> films adsorbed at (a) pH 3.0, (b) pH 5.0, (c) pH 7.0 and (d) pH 9.0. (The Z scale is the same in all figures to facilitate comparison.) RMS values show the root mean square roughnesses.

**Figure S14.** AFM line scans and corresponding images of (PAH/PDCMAA)<sub>10</sub> films adsorbed at (a) pH 3.0, (b) pH 5.0, (c) pH 7.0 and (d) pH 9.0.

**Figure S15.** Sorption isotherms for Cu<sup>2+</sup> binding to (PAH/PDCMAA)<sub>10</sub> at 4, 25 and 37 °C. Films were assembled at pH 3.0, and binding was allowed to occur for 15 h in pH 4.0 solution (20 mM phosphate). The line shows a fit to the data using the Sips isotherm.

**Figure S16.** Sorption isotherms for Cu<sup>2+</sup> binding to (PAH/PDCMAA)<sub>10</sub> at 16 and 31 °C. Films were assembled at pH 3.0, and binding was allowed to occur for 15 h in pH 4.0 solution (20 mM phosphate). The line shows a fit to the data using the Langmuir isotherm.

**Figure S17.** Sorption isotherms for Cu<sup>2+</sup> binding to (PAH/PDCMAA)<sub>10</sub> at 16 and 31 °C. Films were assembled at pH 3.0, and binding was allowed to occur for 15 h in pH 4.0 solution (20 mM phosphate). The line shows a fit to the data using the Sips isotherm.

### **Synthesis of poly[(*N,N*-dicarboxymethyl)allylamine]**

Synthesis of poly[(*N,N*-dicarboxymethyl)allylamine] (PDCMAA) was carried out according to a literature procedure<sup>1</sup> with slight modifications. Under a N<sub>2</sub> atmosphere, chloroacetic acid (6.69 g, 0.07 mol), NaOH (2.80 g, 0.07 mol) and 25 ml of water were added to a two-neck round-bottomed flask, and the mixture was stirred at 30 °C for 10 min. This solution was added

dropwise with stirring to an aqueous solution (100 mL) containing poly(allylamine hydrochloride) (PAH,  $M_n \sim 5.8 \times 10^4$  Da, 1.0 g, 0.011 mol) at 50 °C. The reaction mixture was kept at 50 °C for 1 h and then held at 90 °C for 2 h with occasional addition of 30% NaOH to maintain the pH at 10.0. The reaction mixture was stored at room temperature for 12 h, and then the pH was adjusted to 1 by adding concentrated HCl. The supernatant was decanted, the remaining precipitate was dissolved by addition of 30% NaOH, and the solution was again adjusted to pH 1.0 with concentrated HCl. This process was repeated 2 times, and the precipitate was filtered and dried *in vacuo* for 12 h. The resulting white poly[(*N,N*-dicarboxymethyl)allylamine] (PDCMAA) solid (70% yield) was characterized by  $^1\text{H-NMR}$  (Figure S1b) and FTIR (Figure S2c) spectroscopy. IR (KBr): 1631, 1735 and 1400  $\text{cm}^{-1}$ ;  $^1\text{H-NMR}$   $\delta$  (ppm): 0.50-2.00 (br, s, 3H), 2.00-2.75 (br s, 2H), 2.80-3.50 and (br s, 4H).

The IR spectrum (Figure S2c) of the acidified PDCMAA shows the disappearance of bands that correspond to N-H deformation vibrations of PAH (1510  $\text{cm}^{-1}$  and 1599  $\text{cm}^{-1}$ ) and the appearance of stretches from carboxyl groups. The absorption centered at 1731  $\text{cm}^{-1}$  arises from the C=O stretching in the  $\text{HN}^+\text{-CH}_2\text{COOH}$  group, and the band at 1630  $\text{cm}^{-1}$  is due to the asymmetric stretching in the  $\text{HN}^+\text{-CH}_2\text{COO}^-$  group. The  $^1\text{H-NMR}$  spectrum of PDCMAA shows a signal at  $\delta$  2.80-3.50 corresponding to the  $\text{-NCH}_2\text{COO}^-$  protons. Comparison of the signal integrations for the  $\text{-CH}_2\text{N}$  protons ( $\text{H}_c'$ ) at  $\delta \sim 2.00\text{-}2.75$  ppm and the carboxymethylene protons ( $\text{H}_d$ ) at  $\delta \sim 2.80\text{-}3.50$  ppm suggests that the iminodiacetic moiety is introduced essentially quantitatively into the amino groups of PAH, consistent with previous work.<sup>1</sup>

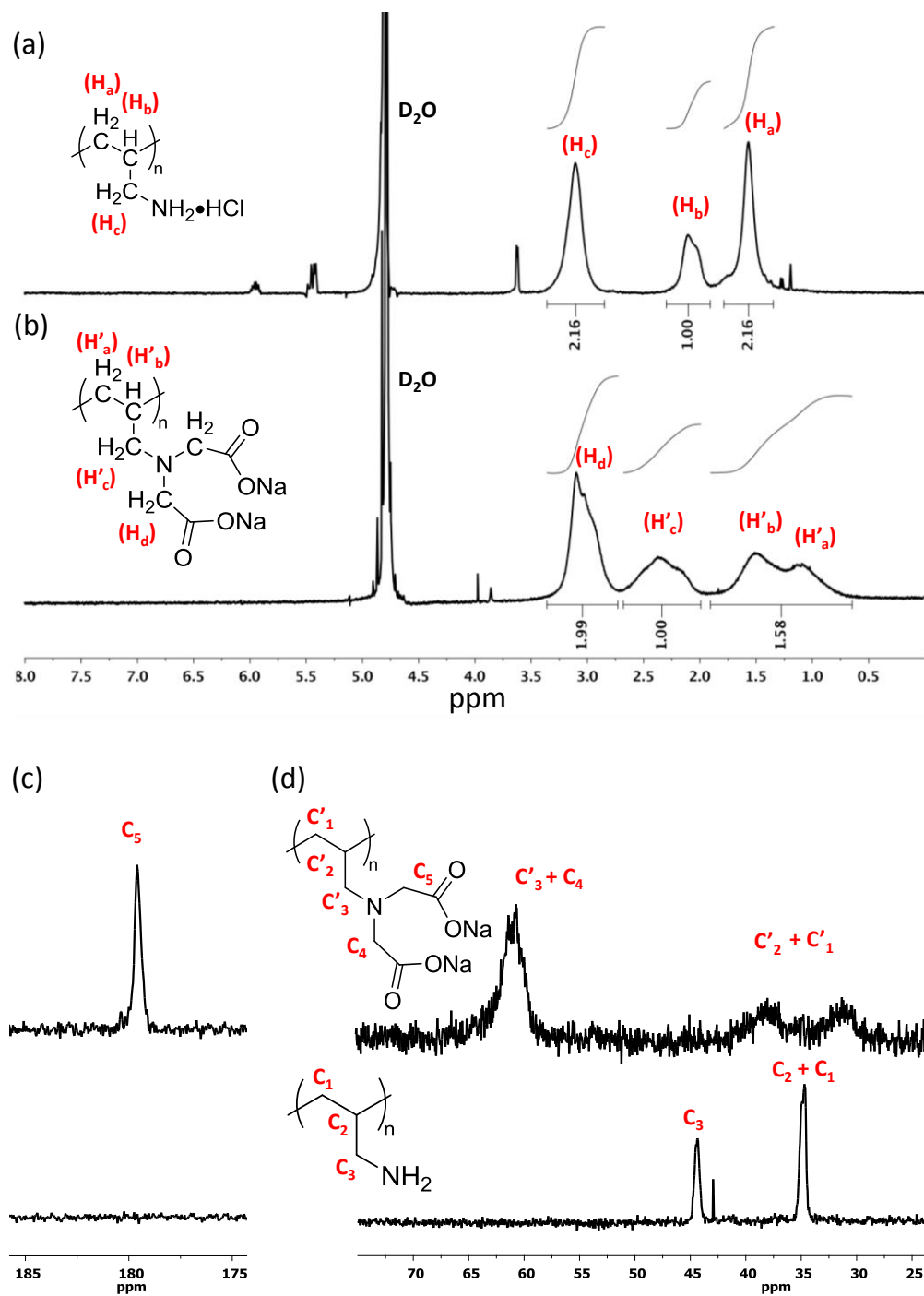


**Figure S1.** <sup>1</sup>H NMR spectra of (a) poly(allylamine hydrochloride) (PAH) in D<sub>2</sub>O and (b) poly[(N,N-dicarboxymethyl)allylamine] in D<sub>2</sub>O adjusted to pH >10 by addition of NaOD. (c) <sup>13</sup>C NMR spectra of PAH (bottom) and PDCMAA (top). Both spectra were acquired in D<sub>2</sub>O adjusted to pH 10 by addition of NaOD. In the <sup>13</sup>C NMR spectrum of PDCMAA, the signals due to the carbons in the polymer backbone are likely low due to restricted relaxation.

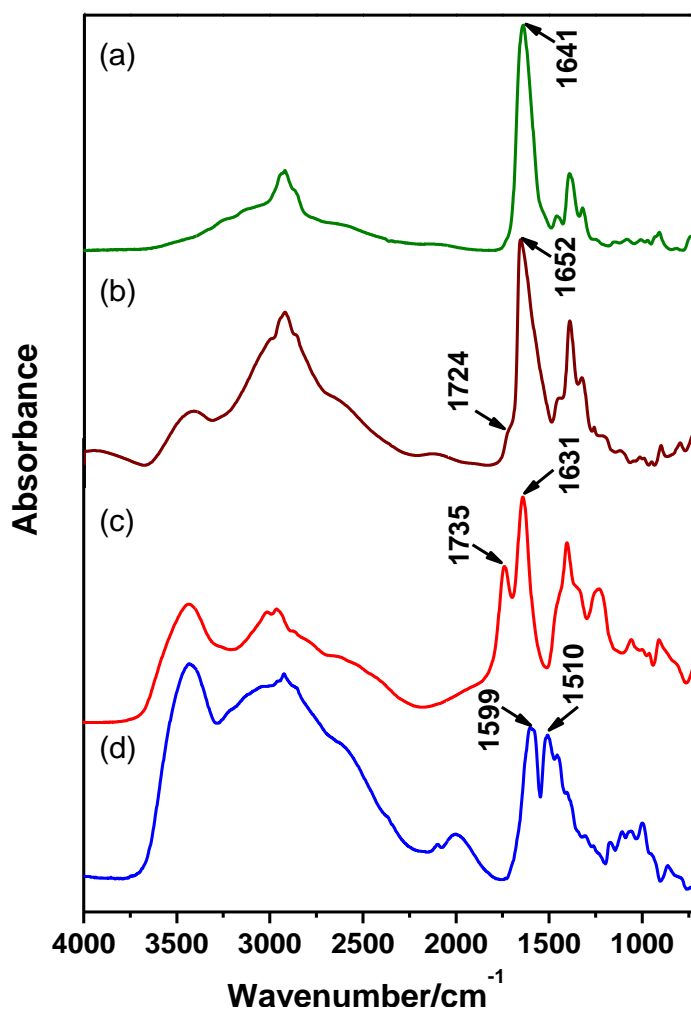


**Figure S2.** IR spectra of (a) a (PAH/PDCMAA)<sub>10</sub>-Cu<sup>2+</sup> film on Au (reflectance spectrum), (b) a (PAH/PDCMAA)<sub>10</sub> film on Au (reflectance spectrum), (c) PDCMAA (in KBr) and (d) PAH (in KBr). Absorbance scales are not the same for all spectra.

### Potentiometric titration of PDCMAA

A potentiometric titration of PDCMAA was performed according to a literature procedure with slight modifications.<sup>1,2</sup> The pH was monitored using a microprocessor-controlled pH-meter (ORION-420A) with a combined glass/reference electrode calibrated with standard pH 4.0, 7.0,

and 10.0 buffers. (Uncertainties in pH values will increase outside of this calibration range.) PDCMAA and PAH were separately dissolved in 0.05 M NaOH, and 1.0 M HCl served as the titrant for 200 mL of ~22 mM PDCMAA or PAH repeating units. Polymer concentrations are likely overestimated because of adsorbed water and Na<sup>+</sup> ions in the PDCMAA. Using a micropipette, the 1.0 M HCl was added in 100-200  $\mu$ L aliquots, except for close to the equivalent point, where 20  $\mu$ L aliquots were added. pH values were recorded after establishing equilibrium, which typically required 1-2 min. Figure S3 shows the resulting acid-base titration curves. For PDCMAA, the first equivalence point occurs around pH 6 after complete protonation of amine groups. Protonation of the two -COOH groups occurs primarily below pH 4. The titration curves agree with literature data.<sup>1-3</sup>

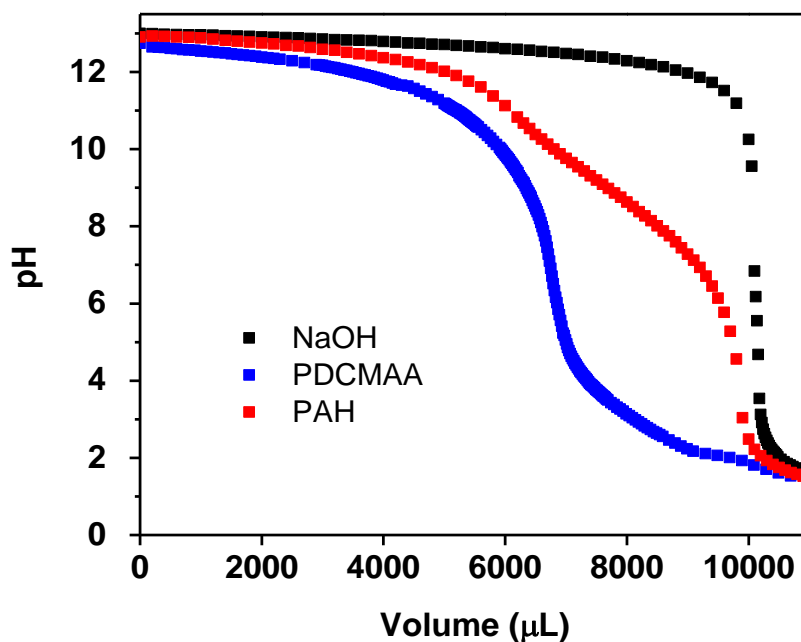


**Figure S3.** Acid-base titration curves for 0.05 M NaOH (black-squares), ~0.022 M PAH in 0.05 M NaOH (red-squares) and ~0.022 M PDCMAA in 0.05 M NaOH (blue-squares). The titrant contained 1.0 M HCl and the initial solution volume was 200 mL.

### Determination of surface energies

Static contact angles were measured with a FirstTenAngstroms (FTA) goniometer. Droplets (~30-40  $\mu\text{L}$ ) of deionized water or ethylene glycol were placed on the surfaces of  $(\text{PAH/PDCMAA})_{10}$  and  $(\text{PAH/PDCMAA})_{10}/\text{PAH}$  films assembled from solutions with various pH values. After a few seconds, droplet images were recorded and subsequently analyzed to determine the contact angle. To minimize variations due to humidity fluctuations, all the measurements were recorded on the same day. Furthermore, another set of films were tested after vacuum drying for 24 h to examine the effect of humidity. Contact angles were determined within 2 min of removing the film from vacuum.

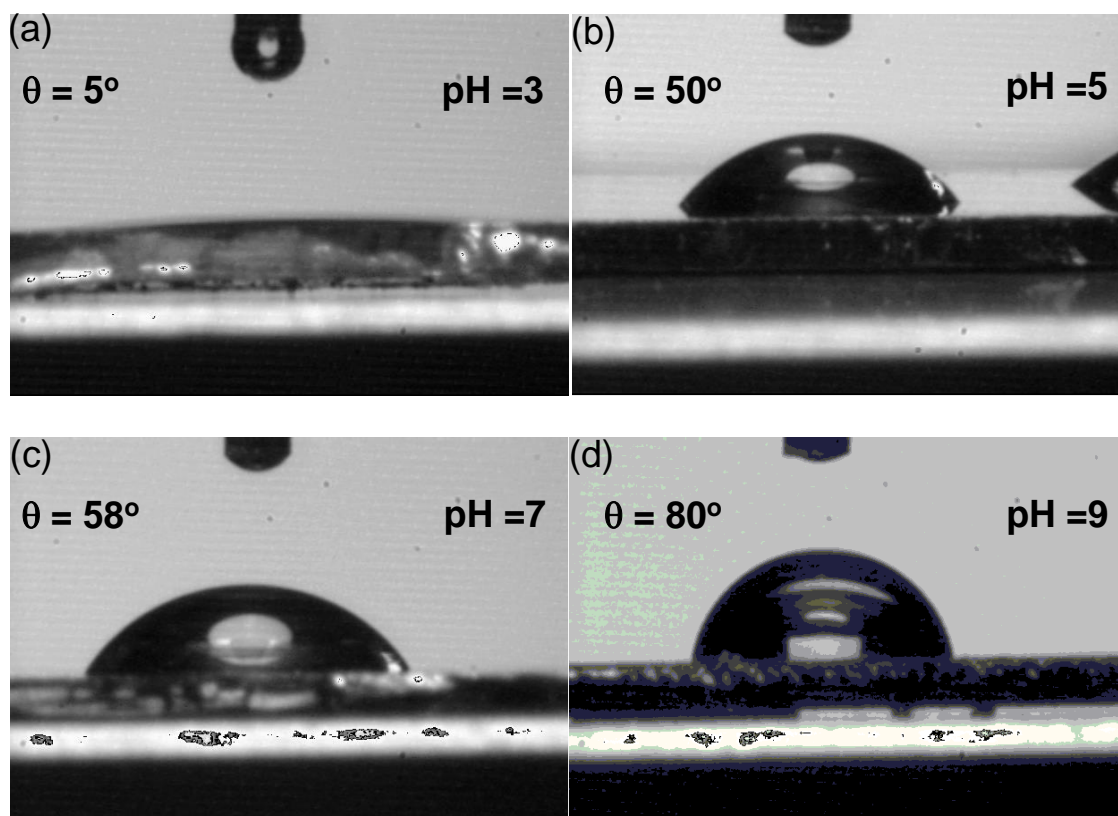


**Figure S4.** Images of water droplets on the surfaces of  $(\text{PAH/PDCMAA})_{10}$  films assembled at pH (a) 3.0, (b) 5.0, (c) 7.0 and (d) 9.0. Values of  $\theta$  represent the average contact angle determined from the image.

**Table S1.** Contact angles on (PAH/PDCMAA)<sub>10</sub> films deposited at different pH values.

Substrate deposition pH	Water Contact angles (°)		Ethylene glycol contact angles (°) <sup>a</sup>
	<sup>a</sup> Films in "ambient air"	<sup>b</sup> Vacuum dried films	
pH 3.0	5.5 ± 0.2	39.2 ± 2.6	15.8 ± 2.7
pH 5.0	50.3 ± 0.4	77.4 ± 4.0	27.2 ± 0.3
pH 7.0	58.4 ± 0.5	76.9 ± 5.5	30.4 ± 2.3
pH 9.0	80.3 ± 0.8	84.9 ± 3.3	43.7 ± 0.7

<sup>a</sup>Films were dried with a stream of N<sub>2</sub> and stored in ambient conditions prior to measurements.

<sup>b</sup>Contact angles were determined after vacuum drying of the film for 24 h.

**Table S2.** Contact angles on (PAH/PDCMAA)<sub>10</sub>/PAH films deposited at different pH values.

Substrate deposition pH	Water Contact angles (°)	
	<sup>a</sup> Films in "ambient air"	<sup>b</sup> Vacuum dried films
pH 3.0	67.7 ± 15.4	82.6 ± 7.1
pH 5.0	71.1 ± 9.5	78.4 ± 4.1
pH 7.0	73.5 ± 13.1	82.4 ± 3.2
pH 9.0	76.2 ± 3.6	85.7 ± 2.7

<sup>a</sup>Films were dried with a stream of N<sub>2</sub> and stored in ambient conditions prior to measurements.

<sup>b</sup>Contact angles were determined after vacuum drying of the film for 24 h.

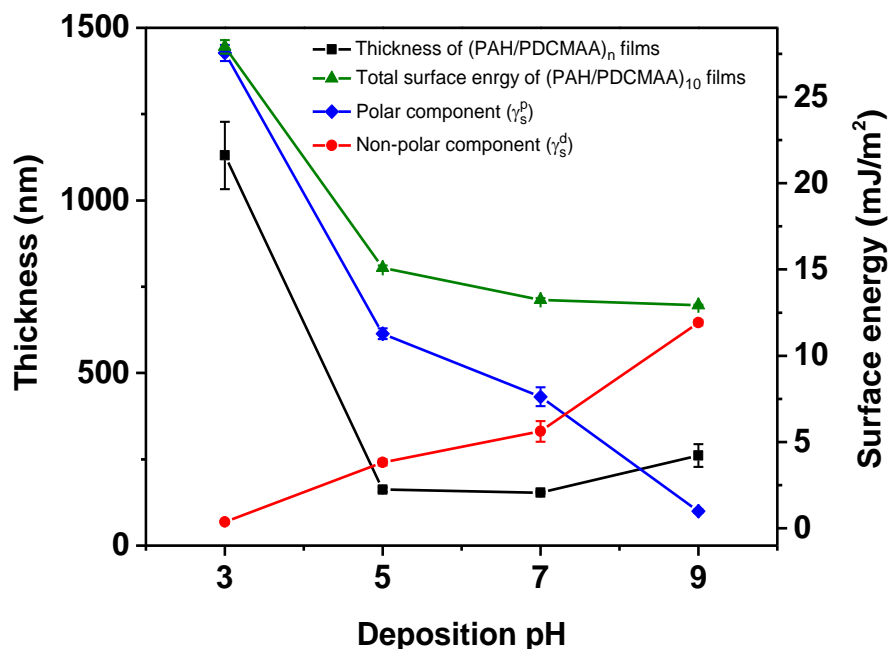


**Figure S5.** Total surface energies, polar ( $\gamma_s^p$ ) and non-polar ( $\gamma_s^d$ ) components of surface energies, and thicknesses of (PAH/PDCMAA)<sub>10</sub> films assembled at different pH values.

Figure S4 shows water contact angles on (PAH/PDCMAA)<sub>10</sub> films deposited at pH 3.0, 5.0, 7.0, and 9.0. The contact angles increase dramatically from a wetted surface for films deposited at pH 3.0 to 80° for films deposited at pH 9.0. To further interrogate surface energies, we employed water and ethylene glycol as reference liquids to determine the polar ( $\gamma_s^p$ ) and the non-polar ( $\gamma_s^d$ ) dispersive components of the surface energy. Table S1 shows the contact angle values on the different films. The observed contact angles were converted to surface energies using Fowkes' equation<sup>4</sup>:

$$\gamma_L(1 + \cos \theta) = 2 \left[ \sqrt{\gamma_L^d \gamma_s^d} + \sqrt{\gamma_L^p \gamma_s^p} \right] \quad (\text{S1})$$

where  $\gamma_L$  is the total surface energy between the droplet and air (for water- 72.8 mJ/m<sup>2</sup> and for ethylene glycol- 48.0 mJ/m<sup>2</sup>),  $\gamma_L^d$  is the dispersive component (for water- 21.8 mJ/m<sup>2</sup> and for ethylene glycol- 29.0 mJ/m<sup>2</sup>), and  $\gamma_L^p$  is the polar component (for water- 51.0 mJ/m<sup>2</sup> and for ethylene glycol- 19.0 mJ/m<sup>2</sup>) of the liquid-vapor surface energies. Application of equation (S1) to each of the probe liquids yields two equations with two unknowns,  $\gamma_s^p$  and  $\gamma_s^d$ , which we obtain from the solution of the two equations. The total energy of the film-air interface,  $\gamma_s$ , is a sum of polar ( $\gamma_s^p$ ) and dispersive ( $\gamma_s^d$ ) surface tensions.

Figure S5 shows  $\gamma_s$ ,  $\gamma_s^p$  and  $\gamma_s^d$  as a function of assembly pH. The PEM deposited at pH 3.0 has the highest total surface energy, and the biggest change in surface energy occurs on increasing the deposition pH from 3.0 to 5.0. Moreover,  $\gamma_s^p$  decreases with the assembly pH, whereas  $\gamma_s^d$  increases. For films deposited at low pH, excess –COOH groups are likely exposed near the interface, and deprotonation of these groups at neutral pH should create a charged, hydrated polar surface. As the deposition pH increases, the films likely expose more and more polymer backbone to decrease  $\gamma_s^p$  and increase  $\gamma_s^d$ .<sup>5</sup> Capping of films by adsorption of a PAH layer gives rise to increased water contact angles when film deposition occurs at pH 3.0, 5.0, and 7.0 (Table S2), confirming the importance of –COO<sup>–</sup> groups in creating a hydrophilic surface. Contact angles increase after vacuum drying of films (Tables S1 and S2) indicating that sorbed water increases hydrophilicity, particularly for films adsorbed at low pH.

### **Film swelling and refractive indices**

The film refractive index is a function of both the constituent polymers and the amount of sorbed water and thus allows estimation of water sorption at ambient conditions.<sup>6,7</sup>

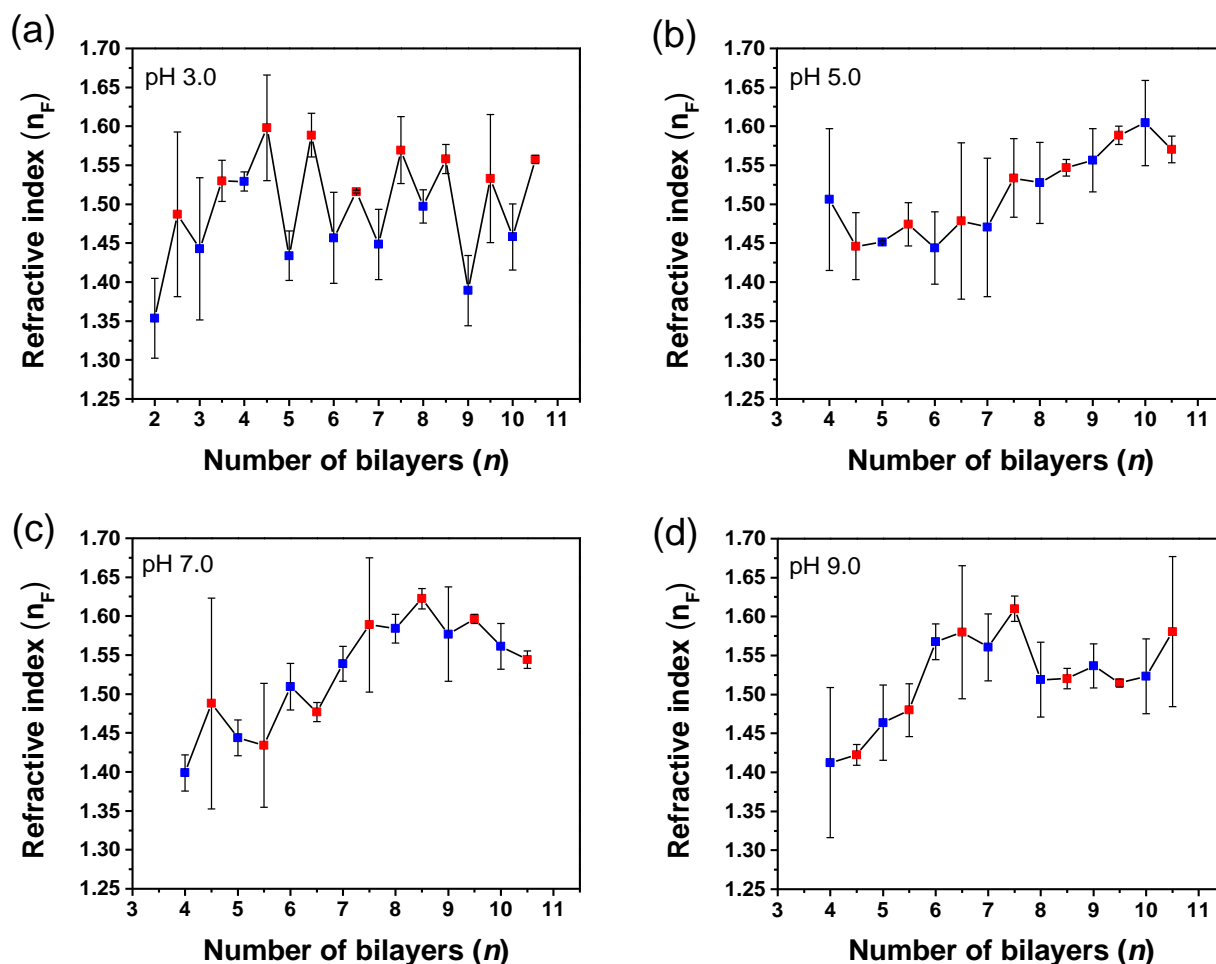
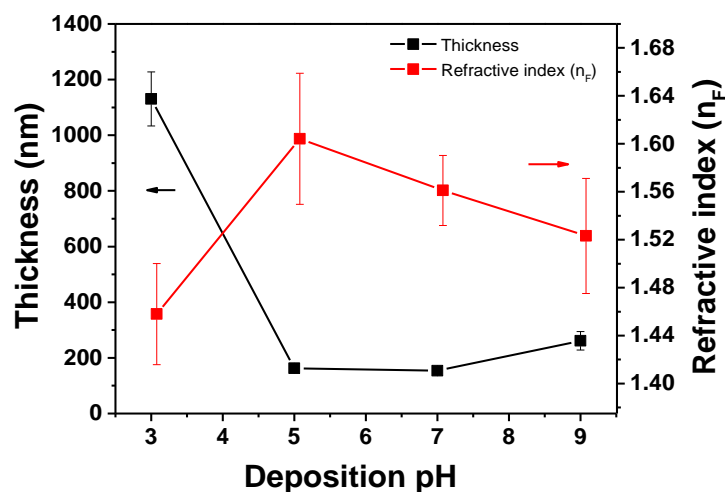


**Figure S6.** Ellipsometrically determined refractive indices (549 nm) for (PAH/PDCMAA)<sub>n</sub> films deposited at pH 3.0, 5.0, 7.0 and 9.0. Integer numbers of bilayers indicate films terminated with PDCMAA deposition (blue squares) and fractional numbers represent terminal PAH deposition (red squares). Films with fewer layers did not give reliable values for refractive indices because of their low thickness.

Figure S6a shows how the refractive index of PAH/PDCMAA films deposited at pH 3.0 varies with the number of adsorbed layers. Despite the uncertainty in the data, in general the refractive index increases after adsorption of PAH and decreases after adsorption of PDCMAA. The multilayers with PDCMAA as the last deposited layer show refractive indices of 1.35-1.53, whereas films ending in PAH deposition exhibit refractive indices from 1.49-1.59. These results

suggest that sorbed PDCMAA at pH 3.0 is more hydrophilic than PAH. During rinsing with water, hydrophilic free  $-\text{COO}^-$  groups form (Figure S12a provides evidence for  $-\text{COO}^-$  groups in films deposited at pH 3.0 and rinsed with water). Adsorption of PAH should lead to complexes of these groups and decrease swelling.

In contrast, the refractive indices of films deposited at pH 5.0, 7.0 and 9.0 show no detectable difference for films terminated with PDCMAA and PAH adsorption. Refractive index values are lower for films with 4~7 bilayers, which may indicate more water in thinner films,<sup>8,9</sup> perhaps because of heterogeneous surface coverage.<sup>7,10</sup> However, the fitted values of refractive indices are less accurate in relatively thin films (Figure S10 gives values of film thicknesses). After adsorption of 10 bilayers, the refractive indices for films deposited at pH 5.0, 7.0, and 9.0 range from 1.52 to 1.59 (Figure S6 b, c & d and Figure S7), which is consistent with values for other polyelectrolyte films.<sup>5</sup>



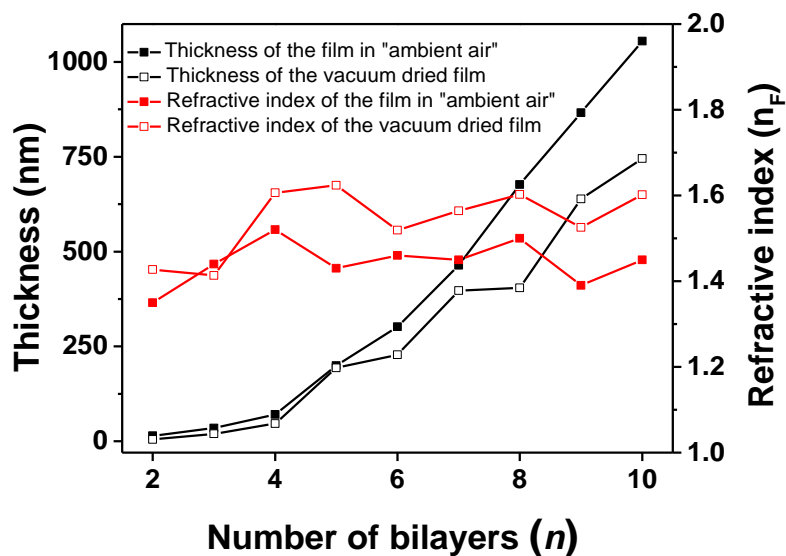
**Figure S7.** Ellipsometric thicknesses and refractive indices (548.8 nm) of  $(\text{PAH/PDCMAA})_{10}$  films assembled at different pH values.

Figure S7 shows the thicknesses and refractive indices of (PAH/PDCMAA)<sub>10</sub> films as a function of the pH of polyelectrolyte deposition solutions. We employed the refractive index values to estimate the water content of the film deposited at pH 3.0.<sup>7,11</sup> Equation (S2) describes the film refractive index,  $n_f$ , as a linear combination of the refractive indices of the polymers,  $n_p$ , and water,  $n_w$ , where  $\phi$  is the volume fraction of polymer in the film. Assuming that the film with the highest refractive index (1.59) contains no water (such a high refractive index is consistent with a non-hydrated polymer),<sup>9</sup>

$$n_f = \phi n_p + (1 - \phi)n_w \quad (\text{S2})$$

this equation suggests that films deposited at pH 3.0 contains about 37% water (the refractive index of water is 1.33). However, even excluding the amount of water absorbed in the film, (PAH/PDCMAA)<sub>10</sub> films deposited at pH 3.0 would still be at least ~3-fold thicker than films deposited at any other pH value (See Figures S7 and S8). Under ambient conditions, the estimated water content for the films deposited at other pH values was <15%.

To further confirm the presence of water in films formed at pH 3.0, we examined their thicknesses and refractive indices after drying in vacuo for 24 h. For films with 4 or more bilayers, the refractive indices of the dried films ranged from 1.52 to 1.62 (Figure S8). Moreover, the thicknesses of films with 6-10 bilayers were 14-40% lower than for films dried briefly with flowing N<sub>2</sub> and stored in ambient conditions.



**Figure S8.** Ellipsometric thicknesses and refractive indices of PAH/PDCMAA films deposited at pH 3.0 and stored in ambient air or dried in vacuo for 24 h. (Thicknesses were measured within 2 min after removing the substrate from the vacuum chamber.)

We also examined film thickness during immersion in a pH 4.0 solution (20 mM phosphate) in an in situ ellipsometry cell. After 10 min of immersion, we determined the swollen thickness, and the swelling percentages using the following equation, where the “dry” thickness refers to the thickness in ambient air.

$$\% \text{ swelling} = \left[ \frac{\text{swollen thickness} - \text{dry thickness}}{\text{dry thickness}} \right] \times 100 \quad (\text{S3})$$

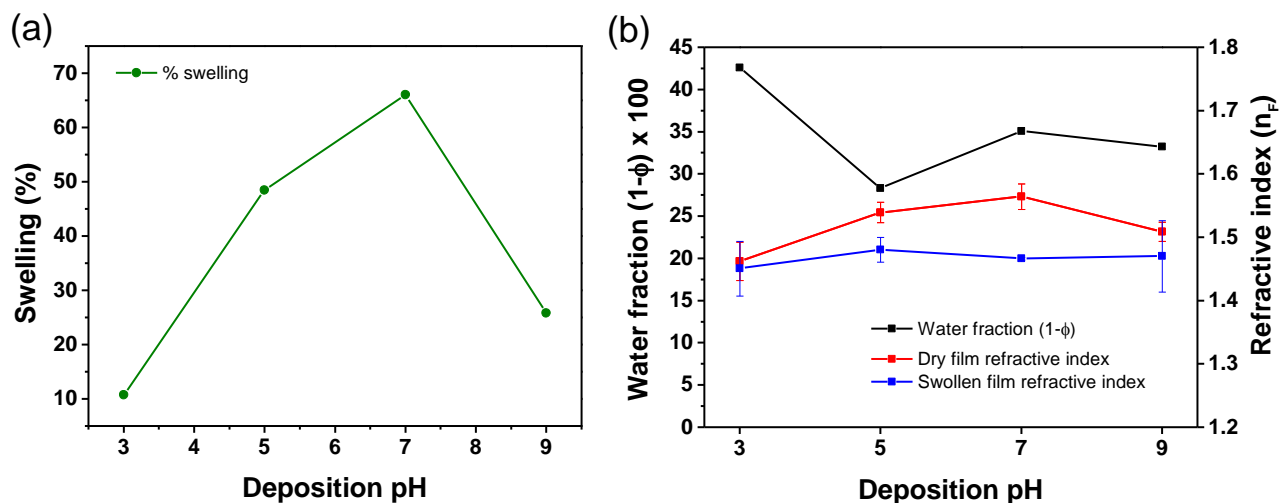


**Figure S9.** (a) Swelling percentages and (b) water volume fractions and refractive indices for (PAH/PDCMAA)<sub>10</sub> films assembled at different pH values and immersed in pH 4.0 water. Figure (b) gives the refractive indices of “dry” films (ambient conditions) for comparison.

Swelling of PAH/PDCMAA films in aqueous solutions will likely affect the rate of Cu<sup>2+</sup> binding. Films assembled at pH 3.0 only swell 10% upon immersion in water, presumably because the “dry” films already contains ~40% water. However, after immersion in water, films deposited at pH 5.0, 7.0 and 9.0 increase in thickness by 48%, 66% and 26%, respectively. Taking into account swelling in the dry films calculated based on refractive indices, films assembled at pH 3.0, 5.0, 7.0, and 9.0 contain 42, 28, 35 and 33 vol% water when immersed in pH 4.0 phosphate solution. The similar refractive indices of all the films immersed in water also suggest similar swelling regardless of deposition pH (Figure S9b). Barrett et al. observed comparable swelling behaviors with PAH/PAA films.<sup>6</sup>

## Film thickness versus the number of adsorbed layers

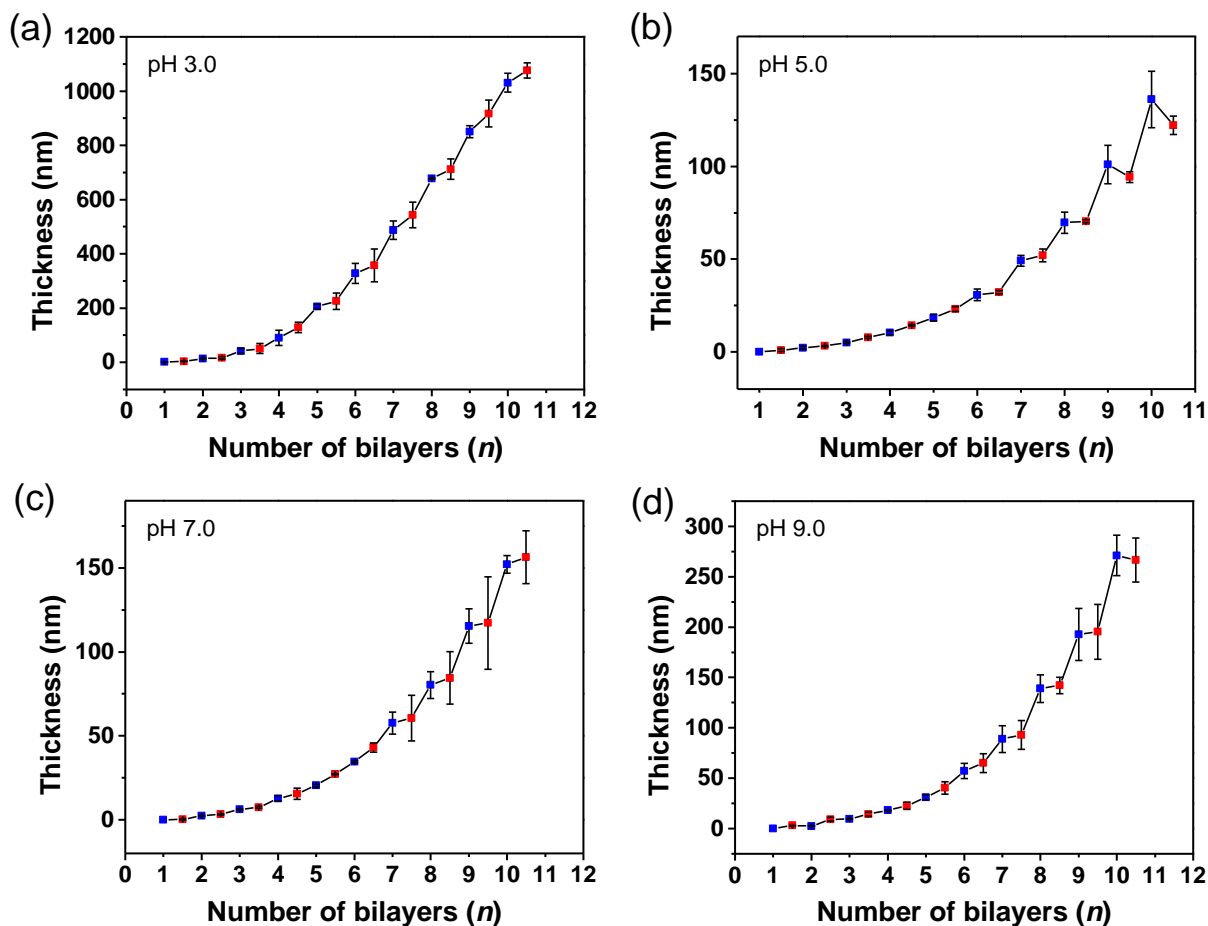


**Figure S10.** “Dry” (ambient conditions) thicknesses of  $(\text{PAH}/\text{PDCMAA})_n$  films adsorbed at (a) pH 3.0, (b) pH 5.0, (c) pH 7.0 and (d) pH 9.0. Fractional values of  $n$  (0.5, 1.5, 2.5, etc.) indicate terminal adsorption of PAH, whereas integers corresponds to terminal adsorption of PDCMAA.

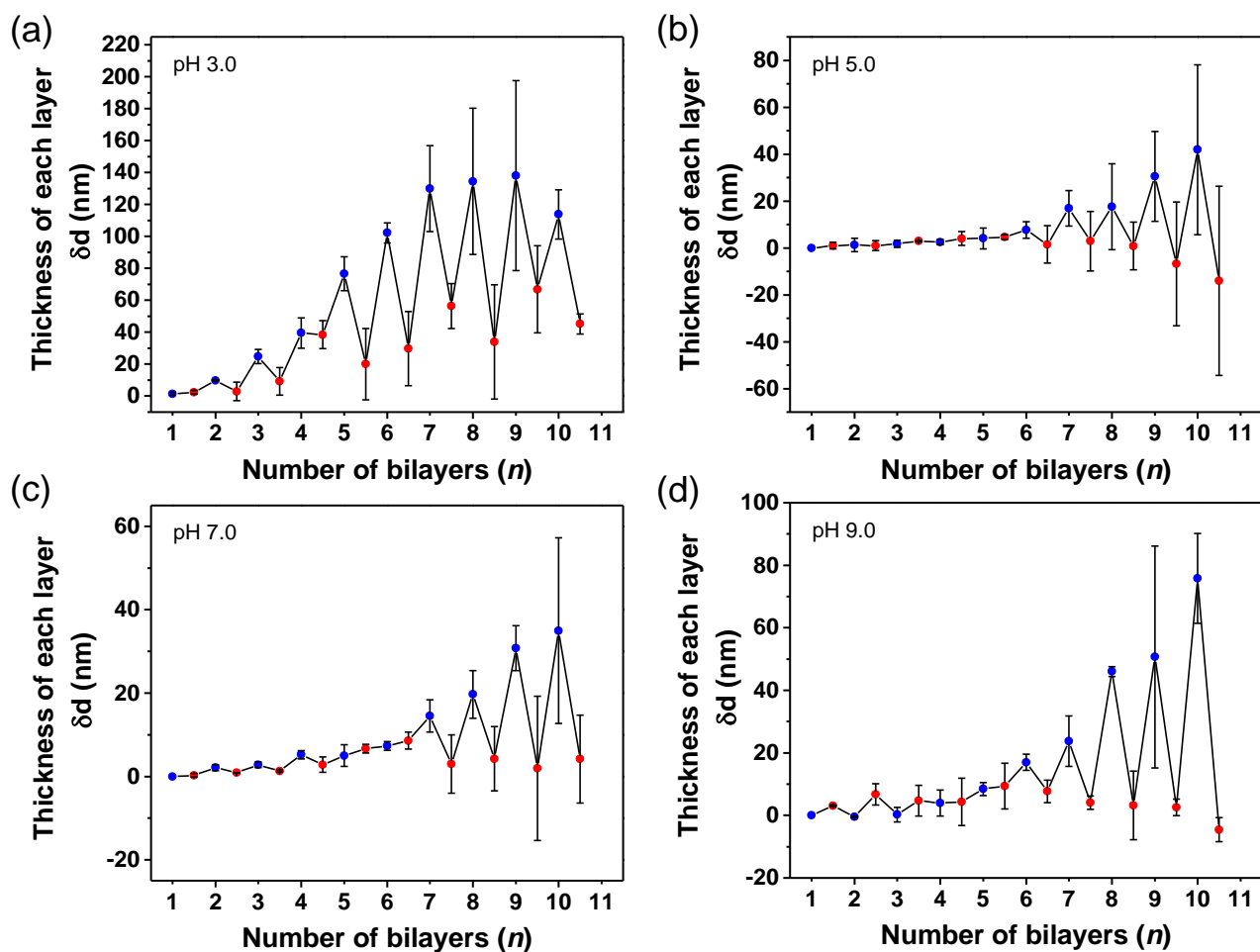


**Figure S11.** Changes in film thickness,  $\delta d$ , after the deposition of each layer in (PAH/PDCMAA)<sub>n</sub> films formed at (a) pH 3.0, (b) pH 5.0, (c) pH 7.0, and (d) pH 9.0. Blue and red circles show the increase in thickness after adsorption of PDCMAA and PAH, respectively.

Figure S10 shows film thickness after each adsorption step in LBL deposition. Reflectance FTIR spectra (Figure S12) show similar increases in absorbance as the number of deposited layers increases. Figure S11 presents the increase in film thickness after deposition of each layer, and Table S3 also provides values of thickness increases after each adsorption step. For deposition at pH 3.0, in the linear range of thickness versus layer number ( $n=5$  to 10), the increases in film thickness after PDCMAA and PAH adsorption range from 77-138 nm and 20-

67 nm, respectively. The greater thickness increase after the PDCMAA deposition step could result from more sorption of PDCMAA than PAH. However, higher swelling of films after PDCMAA sorption also contributes to this thickness increase (see Figure S6a and the discussion of refractive indices).

**Table S3.** Changes in thickness after adsorption of each polyelectrolyte layer during deposition of (PAH/PDCMAA)<sub>n</sub> films at different pH values.\*

Layer number ( <i>n</i> )	Change in thickness (nm) after deposition of each layer			
	pH 3.0	pH 5.0	pH 7.0	pH 9.0
1.5	2.5	1.0	0.3	3.1
2.0	9.8	1.3	2.1	-0.5
2.5	3.0	0.9	0.9	6.7
3	25	1.8	2.8	0.2
3.5	9.3	2.9	1.3	4.7
4	40	2.5	5.2	4.0
4.5	38	4.0	2.8	4.3
5	77	4.0	5.0	8.4
5.5	20	4.7	6.7	9.4
6	102	7.6	7.3	17
6.5	30	1.5	8.6	7.7
7	130	17	14	24
7.5	56	2.9	3.0	4.1
8	134	18	20	46
8.5	34	0.8	4.2	3.2
9	138	31	31	51
9.5	67	-6.8	1.9	2.6
10	114	42	35	76
10.5	45	-14	4.2	-4.6

\*Film thicknesses for 0.5 and 1.0 layer films were below detection.

At deposition pH values of 5.0, 7.0, and 9.0, thickness increases are also greater for PDCMAA than PAH, at least for layers 7-10, and refractive indices are similar for films terminating with PDCMAA and PAH. With deposition at pH 5.0, film thickness even appears to decrease in

some case after the PAH deposition step. Holm et al.<sup>12</sup> suggested that such "odd-even effects" occur because the positively charged polyelectrolyte adsorbs to the surface in a relatively flat conformation. The subsequent PDCMAA deposition may yield complexes with the previously adsorbed PAH layer via coiling of both polymers to give a larger increase in thickness. The relatively low charge density on PDCMAA compared to PAH (at least at pH 5.0) should lead to a more coiled conformation of this polymer and more deposition of PDCMAA than PAH.

### Reflectance IR spectra of (PAH/PDCMAA)<sub>10</sub> films

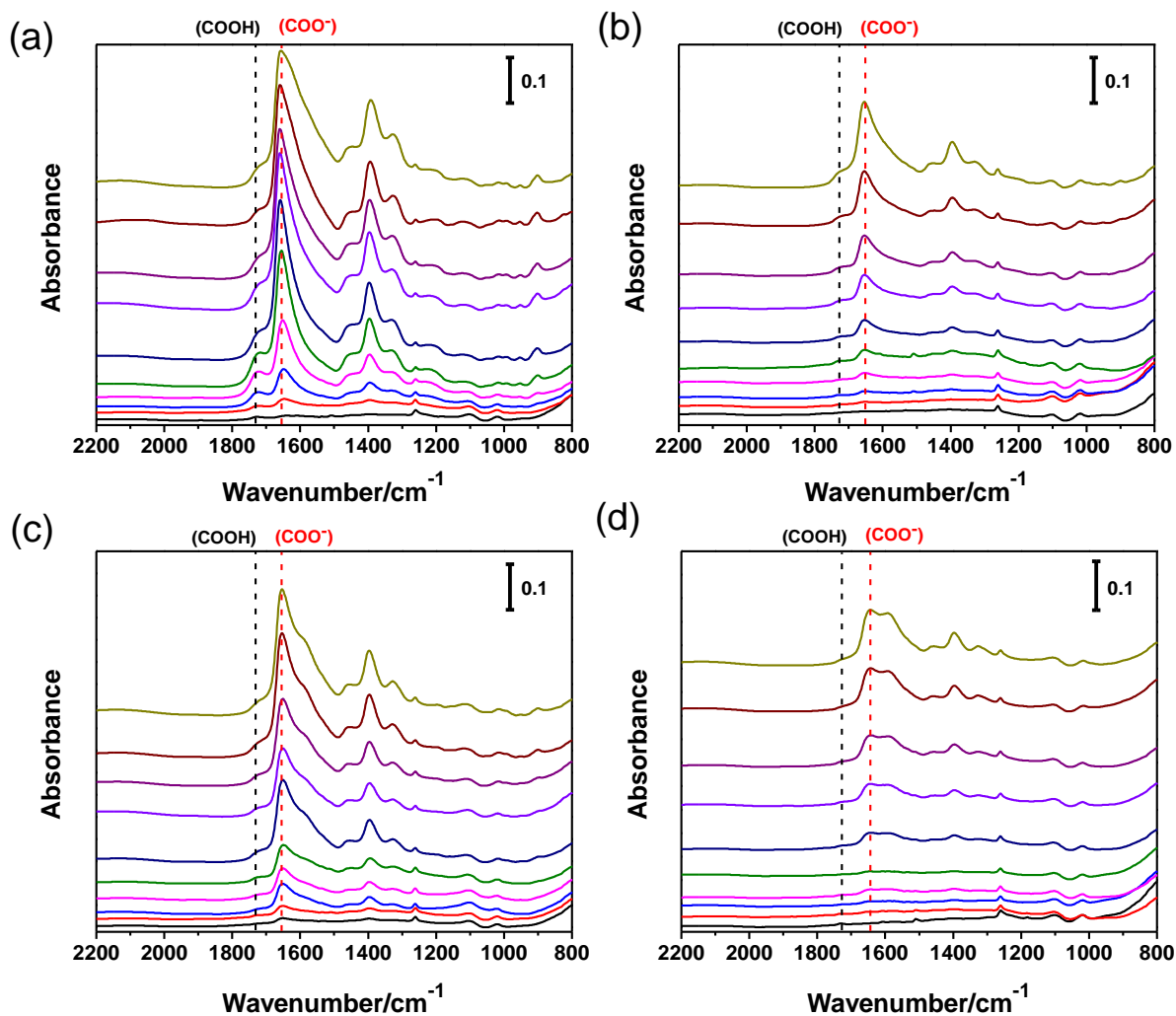


**Figure S12.** Reflectance IR spectra (2200-800 cm<sup>-1</sup>) of (PAH/PDCMAA)<sub>n</sub> films deposited on MPA-modified Au at (a) pH 3.0 (b) pH 5.0, (c) pH 7.0 and (d) pH 9.0. Films were rinsed with deionized water and dried with N<sub>2</sub> prior to obtaining the spectra. In each graph, the number of bilayers in the film increase from  $n=1$  (bottom, black line) to 10 (top, olive green). The large -COO<sup>-</sup> stretch (relative to the acid carbonyl stretch) shows that after rinsing with water most -COOH groups are deprotonated.

### AFM images of (PAH/PDCMAA)<sub>10</sub> films

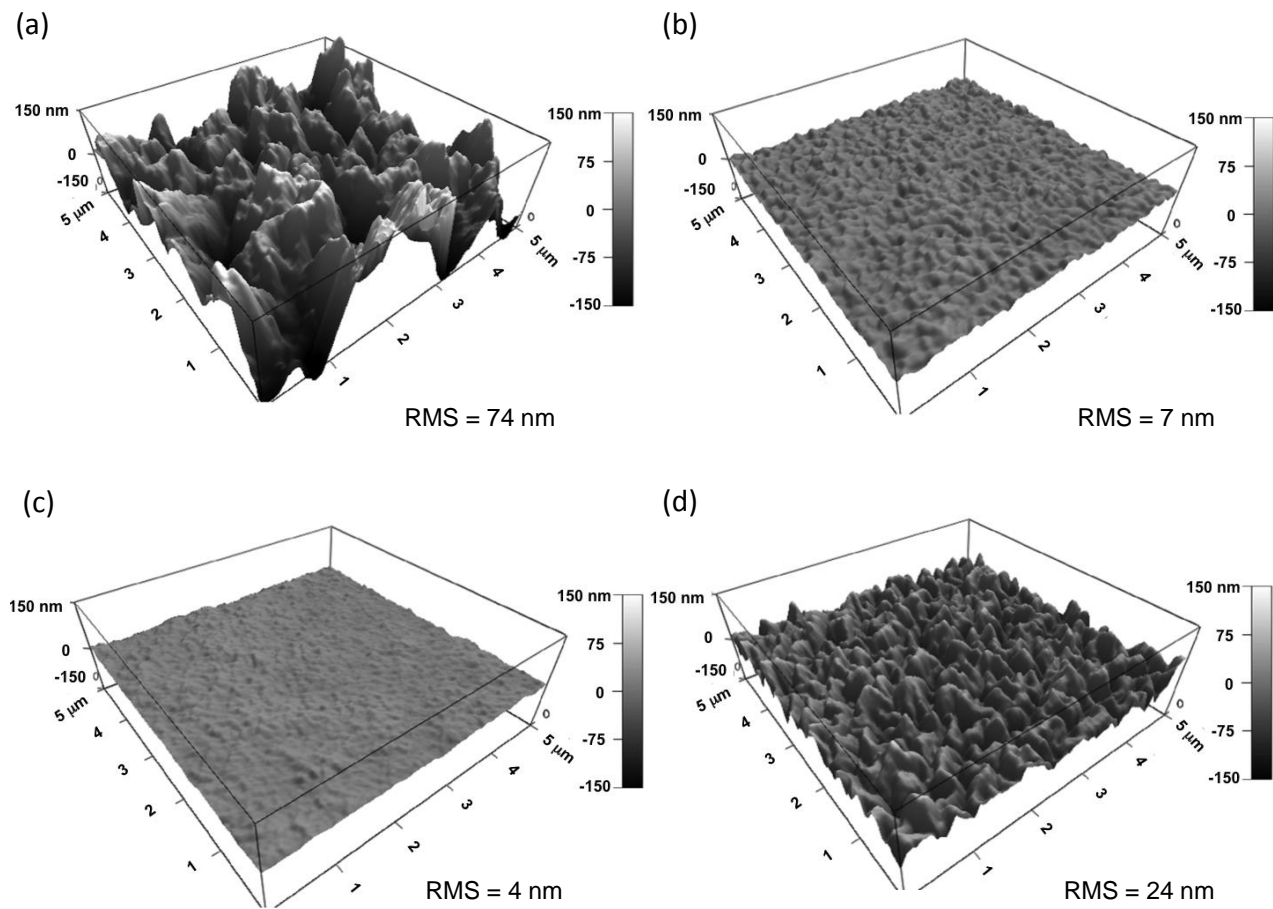


**Figure S13.** AFM 3D images of (PAH/PDCMAA)<sub>10</sub> films adsorbed at (a) pH 3.0, (b) pH 5.0, (c) pH 7.0 and (d) pH 9.0. (The Z scale is the same in all figures to facilitate comparison.) RMS values show the root mean square roughnesses.

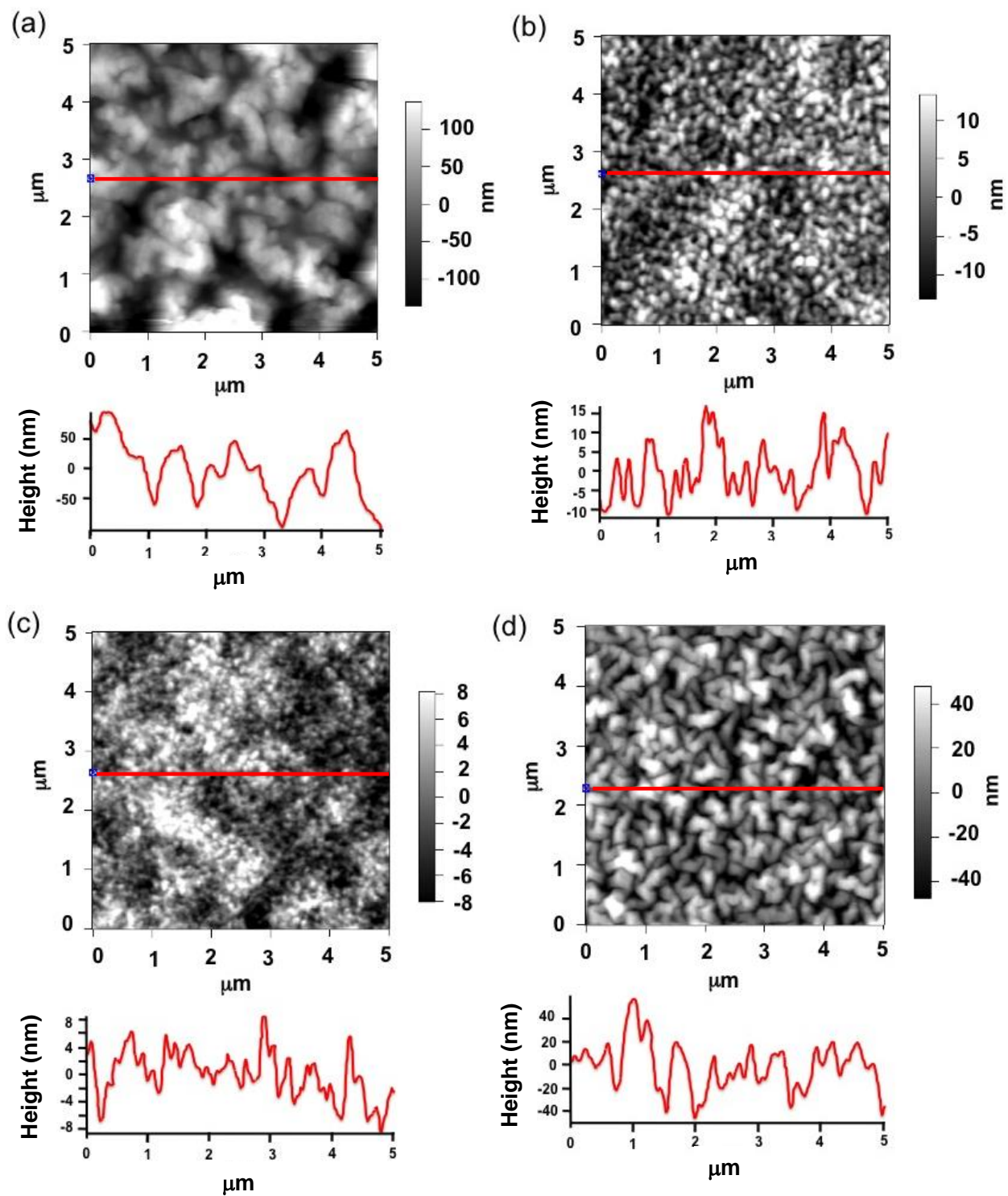


**Figure S14.** AFM line scans and corresponding images of (PAH/PDCMAA)<sub>10</sub> films adsorbed at (a) pH 3.0, (b) pH 5.0, (c) pH 7.0 and (d) pH 9.0.

Sips isotherms for  $\text{Cu}^{2+}$  sorption in  $(\text{PAH/PDCMAA})_{10}$  films at 4, 25 and 37 °C

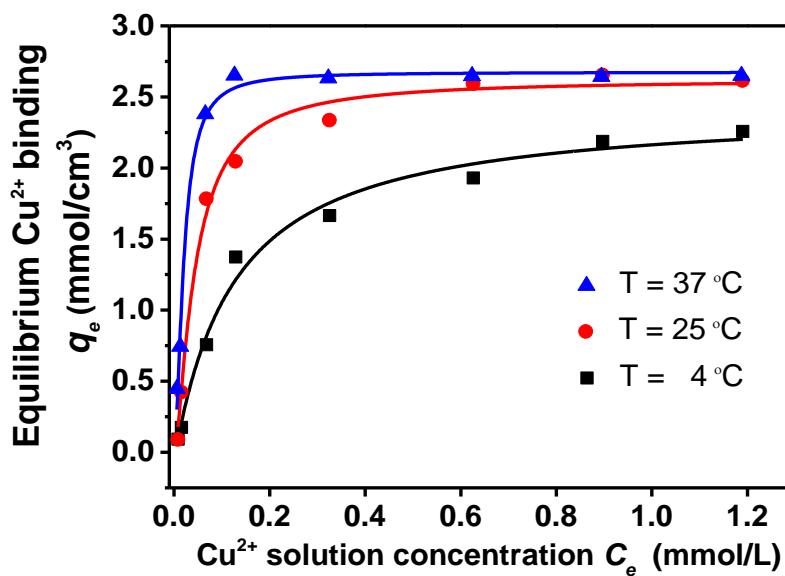


**Figure S15.** Sorption isotherms for  $\text{Cu}^{2+}$  binding to  $(\text{PAH/PDCMAA})_{10}$  at 4, 25 and 37 °C. Films were assembled at pH 3.0, and binding was allowed to occur for 15 h in a pH 4.0 solution (20 mM phosphate). The line shows a fit to the data using the Sips isotherm.

Isotherms for  $\text{Cu}^{2+}$  sorption in  $(\text{PAH/PDCMAA})_{10}$  films at 16 and 31 °C

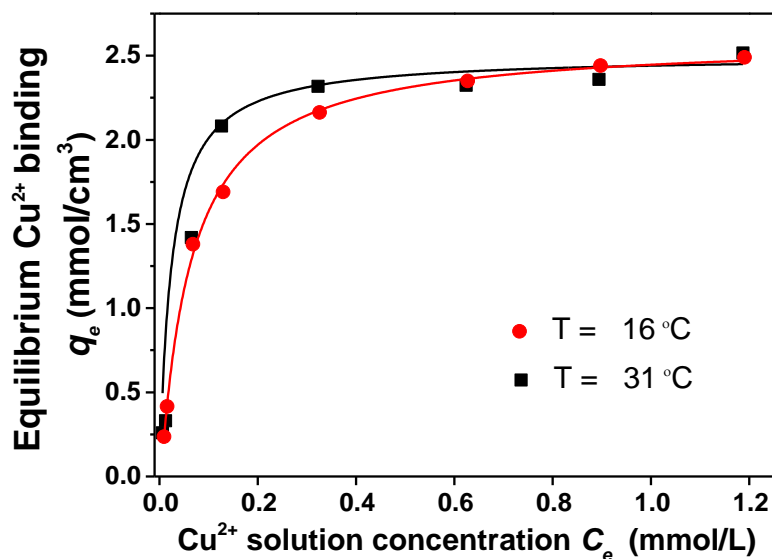


**Figure S16.** Sorption isotherms for  $\text{Cu}^{2+}$  binding to  $(\text{PAH/PDCMAA})_{10}$  at 16 and 31 °C. Films were assembled at pH 3.0, and binding was allowed to occur for 15 h in pH 4.0 solution (20 mM phosphate). The line shows a fit to the data using the Langmuir isotherm.

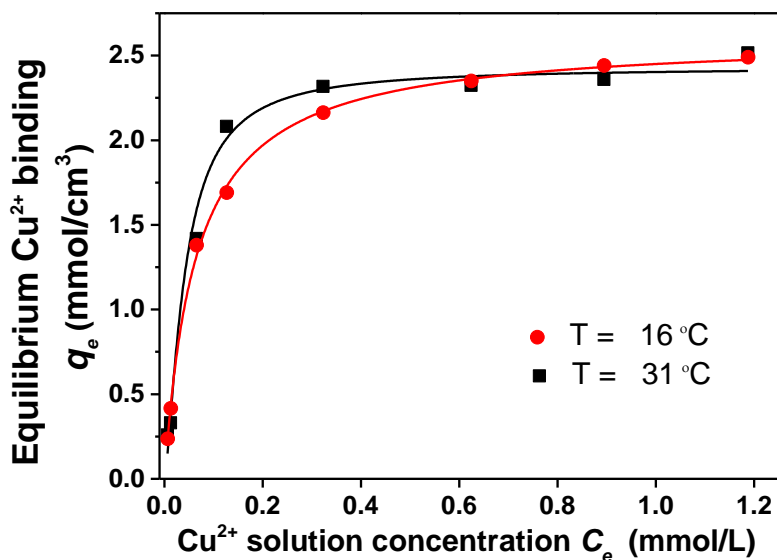


**Figure S17.** Sorption isotherms for  $\text{Cu}^{2+}$  binding to  $(\text{PAH/PDCMAA})_{10}$  at 16 and 31 °C. Films were assembled at pH 3.0, and binding was allowed to occur for 15 h in pH 4.0 solution (20 mM phosphate). The line shows a fit to the data using the Sips isotherm.

## References

- (1) Naka, K.; Tachiyama, Y.; Hagihara, K.; Tanaka, Y.; Yoshimoto, M.; Ohki, A.; Maeda, S. Synthesis and Chelating Properties of Poly (N,N-Dicarboxymethyl)Allylamine Derived from Poly(Allylamine). *Polym. Bull.* **1995**, *35*, 659-663.
- (2) Petrov, A. I.; Antipov, A. A.; Sukhorukov, G. B. Base-Acid Equilibria in Polyelectrolyte Systems: From Weak Polyelectrolytes to Interpolyelectrolyte Complexes and Multilayered Polyelectrolyte Shells. *Macromolecules* **2003**, *36*, 10079-10086.
- (3) Choi, J.; Rubner, M. F. Influence of the Degree of Ionization on Weak Polyelectrolyte Multilayer Assembly. *Macromolecules* **2005**, *38*, 116-124.
- (4) Fowkes, F. M. Attractive Forces at Interfaces. *Ind. Eng. Chem.* **1964**, *56*, 40-52.
- (5) Sailer, M.; Barrett, C. J. Fabrication of Two-Dimensional Gradient Layer-by-Layer Films for Combinatorial Biosurface Studies. *Macromolecules* **2012**, *45*, 5704-5711.
- (6) Tanchak, O. M.; Barrett, C. J. Swelling Dynamics of Multilayer Films of Weak Polyelectrolytes. *Chem. Mater.* **2004**, *16*, 2734-2739
- (7) Halthur, T. J.; Elofsson, U. M. Multilayers of Charged Polypeptides as Studied by in Situ Ellipsometry and Quartz Crystal Microbalance with Dissipation. *Langmuir* **2004**, *20*, 1739-1745.
- (8) Tanchak, O. M.; Yager, K. G.; Fritzsche, H.; Harroun, T.; Katsaras, J.; Barrett, C. J. Water Distribution in Multilayers of Weak Polyelectrolytes. *Langmuir* **2006**, *22*, 5137-5143.
- (9) Wong, J. E.; Rehfeldt, F.; Hanni, P.; Tanaka, M.; Klitzing, R. V. Swelling Behavior of Polyelectrolyte Multilayers in Saturated Water Vapor. *Macromolecules* **2004**, *37*, 7285-7289.
- (10) Schönhoff, M.; Ball, V.; Bausch, A. R.; Dejugnat, C.; Delorme, N.; Glinel, K.; Klitzing, R. V.; Steitz, R. Hydration and Internal Properties of Polyelectrolyte Multilayers. *Colloid. Surface. A* **2007**, *303*, 14-29.
- (11) Ball, V.; Ramsden, J. J. Buffer Dependence of Refractive Index Increments of Protein Solutions. *Biopolymers* **1998**, *46*, 489-492.
- (12) Messina, R.; Holm, C.; Kremer, K. Polyelectrolyte Multilayering on a Charged Sphere. *Langmuir* **2003**, *19*, 4473-4482